Invited Paper

Terahertz tomography

Liting Niu [1, 2], Kejia Wang [1], Zhengang Yang [1], and Jinsong Liu [1*]
[1] Huazhong University of Science and Technology, Wuhan national laboratory for optoelectronics, No. 1037 Luoyu Rd., Wuhan, Hubei, China
[2] Guangdong University of Petrochemical Technology, College of Science, No.139 Guandu 2nd Rd., Maoming, Guangdong, China
[*1] Email: jsliu4508@vip.sina.com

(Received September 18 2019)

Abstract: Terahertz (THz) imaging has greatly progressed over the past two decades because of the advantages of penetrativity, lower optical phantom and broadband. In this paper, we mainly introduce THz computed tomography (CT) and THz time-of-flight (TOF) imaging. Specially, the development of these two kinds of imaging techniques could be classified to some branches. One important branch is reducing the data acquisition time by 2D free-space electro-optic sampling (2D-FSEOS), asynchronous optical sampling (ASOPS) or electronically controlled optical sampling (ECOPS). Another important branch is enhancing the image resolution and quality by optimized reconstruction algorithms. The image quality also could be improved by considering Gaussian beam propagation or replacing the Gaussian beam by a zero-order Bessel beam. Moreover, application investigations of THz CT and THz TOF imaging in different fields such as art conservation, medicine detection, defect identification, industrial inspection are demonstrated and summarized.

Keywords: Terahertz spectral computed tomography, Terahertz continuous-wave computed tomography, Terahertz time-of flight imaging

doi: 10.11906/TST.077-092.2019.09.08

1. Introduction

Various regions of the electromagnetic spectrum have been widely developed in the imaging field, such as microwave, infrared wave, visible light, X-ray and γ ray. The electromagnetic spectrum in different ranges has their own shortcomings. For example, X-ray and γ ray will introduce ionization reaction, which is harmful to the organisms. The visible light and infrared light would be attenuated quickly when they incident on many kinds of materials. The microwave imagers have poorer resolution capabilities because of the long wavelength.

Terahertz (THz) wave bridges the gap between infrared and microwave frequencies, which can penetrate various dielectric materials. The imagers will demonstrate a more vividly images of the detected sample when THz wave is chosen to replace the microwave used in the equipment. THz imagers are alternative techniques for many fields thanks to the better penetration depth than the visible light and infrared wave, such as non-destructive testing (NDT), security imaging, biomedical investigations and semiconductor characterization.

The THz imaging techniques can be classified to be active ones and passive ones according to the involving of transmitter. Here, passive THz imaging techniques can detect the THz wave that are emitted by cosmic dust and gaseous nebulace [1], which is crucial for astronomy. The active imaging techniques can be classified to be pulsed mode and continuous-wave mode based on the generation and detection method of THz wave. According to the detection region, pulsed THz imaging techniques can be classified to be near-field imaging techniques and far-field imaging techniques. The near-field imaging, utilizing localized THz wave, detects the area that is only at the wavelength or sub-wavelength scale from the surface of the sample by raster scanning, and reconstruct the images by acquiring and processing the information of all the points that lie in the detection area. The resolution of near-field imaging mainly depends on the size of the aperture or the pinhole diameter, which can be free from the diffraction limit. Hence, the near-field THz imaging has attracted extensive research efforts of the obtained finer images with a resolution of submicron or even nano-level [2]. Classic far-field imaging technologies with pulsed mode involving 2D transmission method, 2D reflection method, THz binary lens tomography, time-of-flight (TOF) imaging, diffraction tomography, transmission computed tomography (CT) and reflection CT. Common far-field imaging technologies with continuous-wave mode involving 2D transmission method, 2D reflection method, CT, frequency-modulated continuous-wave (FMCW) technology, synthetic aperture radar (SAR) and single-pixel imaging method. In the aforementioned, THz CT and THz TOF imaging techniques are attracting increasing attention of researchers for the potential applications in nondestructive mail and packaging inspection, semiconductor testing, and manufacturing quality control [3, 4]. Hereinafter, we introduce the development of these two imaging techniques.

2. THz computed tomography

X-ray CT is generally applied for industrial inspection and medical diagnoses. It is an effective method for identifying the sample's internal structure. However, the photon energy of X-ray is high enough to generate ionization reaction. In 2002, transmission THz spectral CT was proposed by B. Ferguson and X-C Zhang [3], which draws inspiration from the now ubiquitous x-ray CT system and is safe because of the low photon energy. The experimental setup is shown in Fig. 1(a), THz pulse (THz beam) is generated by a regeneratively amplified Ti: sapphire laser that incident upon a 14-*mm*-wide aperture photoconductive antenna, which is focused by off-axis parabolic mirrors and guided to the sample. The transmitted THz pulse is collected again and focused onto a ZnTe electro-optic (EO) crystal. The probe pulse is modulated by the THz pulse via the EO effect and is received with the spectrometer and a CCD camera. The collected data are projections to reconstruct the spatial distribution of the absorption coefficient, the refractive index and the material. The picture of a turkey bone is shown in Fig. 1(b) and the corresponding amplitude reconstruction is demonstrated in Fig. 1(c). Clearly, the outer profiles of turkey bone are recognizable, but the fine internal structures are not recovered, which may be because of the beam scattering introduced by the complex structure or the lower spatial resolution.

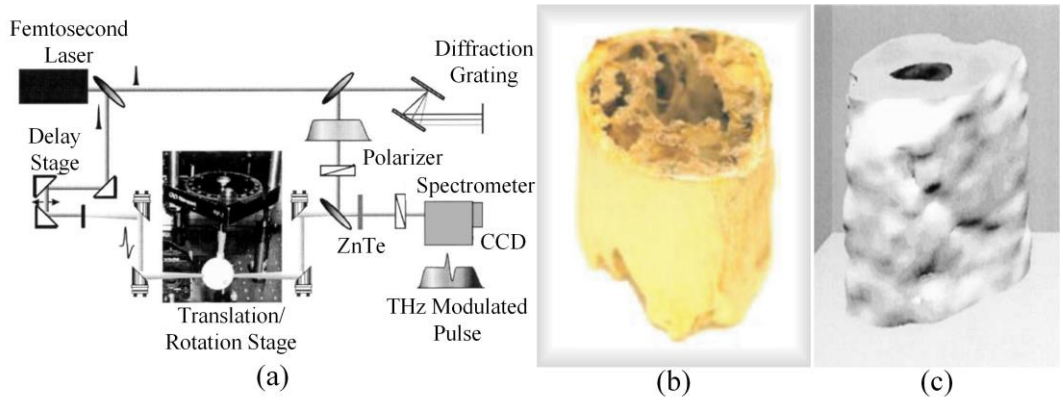

Fig. 1 (a) Experimental setup of THz spectral CT, (b) picture of turkey bone, (c) 3D image reconstructed by FBP algorithm [1].

Compared with the conventional X-ray CT, transmission THz spectral CT can determine the material composition and the structure. The above investigation demonstrates the great potential of THz spectral CT for nondestructive mail and packaging inspection, semiconductor testing, and manufacturing quality control [3]. The applications of THz CT in different fields are investigated since it is proposed. For example, A. Emmanuel and his team tried to investigate the dried human bones such as a lumbar vertebra, a coxal bone, and a skull by CW THz CT and performed a comparison with standard radiography, which demonstrated that THz radiation can differentiate the two types of osseous tissues such as compact and spongy bones [5]. Subsequently, gelatin soluble capsule enclosing a dose of medicine powder is imaged by the CW THz CT, which demonstrated the potential in medical applications [6]. The images of Egyptian jar obtained by THz CT demonstrated the potential in art conservation [7]. The imaging of foam materials by THz CT, which are utilized as thermal protection on the external fuel tanks for the Space Shuttle, demonstrate the potential in aerospace application [8]. The imaging of pencil [9], a straw [10], a dried heart pea, a doll in the egg shell [11], glucose, lactose [12], Teflon [11, 12], and a range of phantoms made form expanded polystyrene [11] and polystyrene [11, 13] demonstrate the potential in industrial inspection. The Advantest corporation have developed the “3D Imaging Analysis System” that uses terahertz pulses, which is the world's first such system for nondestructive three-dimensional spectroscopic analysis of the spatial distribution of constituents in practical applications [14].

2.1 Fast THz computed tomography

The transmission THz spectral CT mentioned above has a strong limitation which is the long data acquisition time arising from time-delay scanning due to the reciprocating motion of a mechanical stage. To reduce the acquisition time, M. Jewariya and E. Abraham et al. proposed fast 3D THz spectral CT based on the real-time 2D free-space electro-optics sampling (2D-FSEOS) [15]. The typical experimental setup is shown in Fig. 2. It takes only 10 *ms* to get the projections of one angle and 6 seconds to get the sinogram of a slice that includes 600 projections.

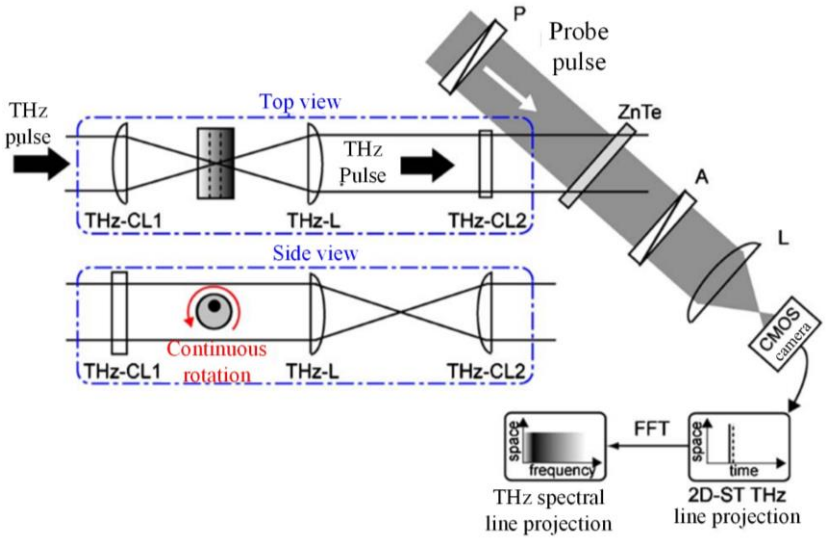

Fig. 2 Fast THz spectral CT base on 2D-FSEOS, THz-CL1 and THz-CL2: cylindrical lens, THz-L and L:plano-convex lenses, P: polarizer, A: analyzer

Asynchronous optical sampling (ASOPS) is another promising method to reduce the data acquisition time [16]. The fast 3D THz spectral CT based on 2D-FSEOS [15] or asynchronous optical sampling (ASOPS) [16] has the ability of identifying chemical component and spatial structure. However, the imaging system has a complicated structure for the large number of optical elements. In addition, it is expensive because of the demand for a femtosecond laser. Hence, continuous-wave THz CT would be a better choice when the internal material of the sample is not necessary to be determined, which has the advantages of low cost and simple structure. In 2013, H.-W. Hübers et al. proposed a continuous-wave THz CT with a scanning mirror, as shown in Fig. 3. The emitted THz beam is collimated by a poly-4-methylpentene-1 (TPX) lens and then is guided to a flat two-axes scanning mirror. The mirror deflects the beam toward a high-density polyethylene (HDPE) lens, which focuses the beam onto the object. By steering the mirror, the beam waist is spirally scanned across the object. The transmitted THz beam is coupled into the detector by an off-axis parabolic mirror. The size of the measurement volume is determined by the field-of-view of the two-dimensional images. An ellipsoidal volume with axes of about 40 *mm* can be measured by the system. The total acquisition time of one three-dimensional image takes only 87 *s*, which are reconstructed from 60 2D images covering a total of 180 ° in steps of 3 ° [17]. The tomosynthesis [18] is another method to reduce data acquisition time for it can reconstruct the images from only a much smaller number of projections. In 2018, T. Mohr et al proposed a CW THz CT that combined with single-pixel imaging technology, which replaces the typical raster-scanning method, can effectively reduce data acquisition time [19].

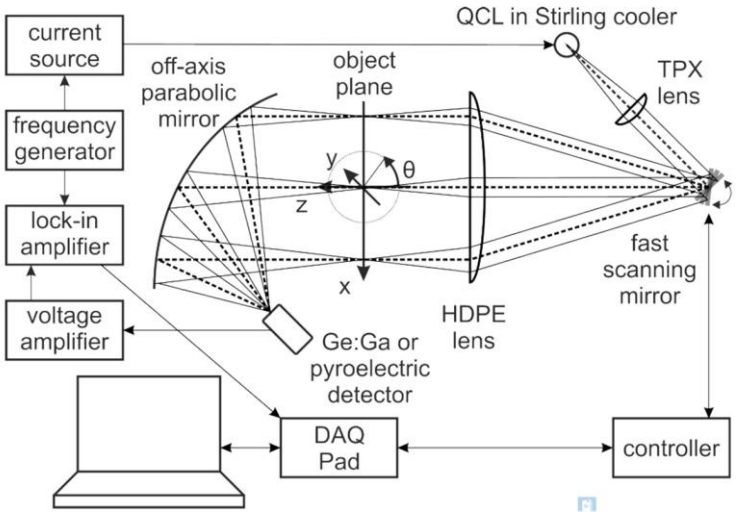

Fig. 3 Fast CW THz CT with scanning mirror

2.2 Optical effects in THz computed tomography

The diffraction effects and Fresnel losses can be neglected when the sample owns lower refractive index or structure characteristics greater than the wavelength [3]. However, they cannot be ignored as soon as the refractive index of the sample is in the order or greater than 1.5 or the complex structure [20, 21]. To solve the issue, E. Abraham et al. introduce a multi-peak averaging method to eliminate boundary effects due to refraction losses of the THz beam inside the material and reconstruct the amplitude and time cross-sections of the samples [20]. Besides, they proposed a correction algorithm for cylindrically shaped objects [22]. The algorithm corrects the edges of the projection data for the finite THz beam size as well as beam steering and Fresnel reflection losses. When the algorithms are applied to plastic rods, the artificially large attenuation near the boundary of the cylindrical sample is removed. However, this method is ineffective for complex sample. A. Brahm et al. measured the intensity distribution of THz beam transmitted through rectangular and cylindrical samples made of PEEK (Polyetheretherketon), POM (Polyoxymethylen), and PMMA (Polymethylmethacrylat) by a geometrical optical ray tracing approach to analyze the optical effects and compared the results to simulations that are realized with the software ZEMAX [21]. This investigation demonstrated that the signal loss are not only refraction effects which are dominant but also diffraction and edge effects, as well as signal offsets that come from noise which are affecting the measurements. Accordingly, new algorithms that combine the beam propagation and the sample's structure should be developed to reduce artifacts of images introduced by optical effects and improve the image quality.

Earlier this year, A new model for the interaction between radiation and objects is investigated. The interaction model is based on a Monte Carlo extension of usual ray tracing methods [23]. It aims to account for the Gaussian intensity profile of the THz beam and considers refraction and reflection losses when propagating through an object. Based on this way, we can effectively eliminate the refractive loss of the reconstructed image in the future. However, it will naturally

induce a more complex model and eventually a more complex reconstruction algorithm.

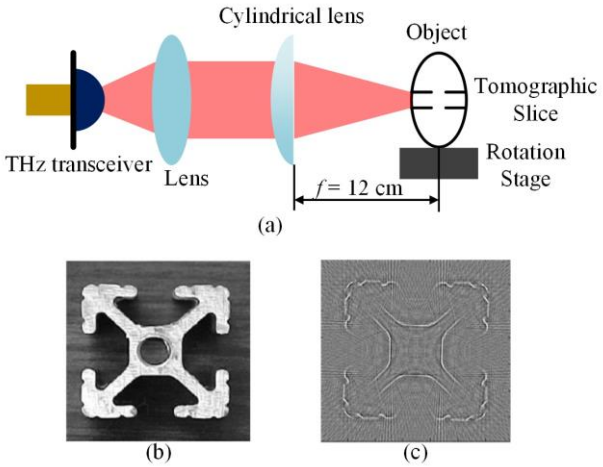

Fig. 4 (a) the experimental setup of reflection THz spectral CT, (b) top view of the cylindrical metal post, (c) the reconstruction image of the cross-section

2.3 Reflection THz computed tomography

For many imaging applications using terahertz (THz) radiation, it is desirable to work in a reflection mode, especially in situations when only one side of the object is accessible to detectors or when the object is opaque. For example, reflection THz CT is a better choice to obtain the external structure of a cylindrical metal post [24]. The reflection THz CT system is shown in Fig. 4(a), the THz pulse emitted by transceiver is collimated by a lens, and then it is focused to a horizontal line using a cylindrical lens (focal length 12 *cm*) to restrict the illumination of the object to a thin horizontal slice as illustrated by the dashed lines. The reflected THz pulse is converged by two lens and collected by transceiver [24]. The object is rotated in 1 ° increments over 360 ° to obtain the sinogram of the tomographic slice and reconstruct the images by using FBP algorithm. The top view of the cylindrical metal post and the reconstructed image of the cross-section are presented in Fig. 4(b) and (c) respectively. Notably, void inside the metal post and the edge blocked by the metal cannot be obtained in the reconstructed image because the terahertz wave cannot pass through the metal.

2.4 Reconstruction methods

Common algorithms used in THz CT is Filtered Back-Projection (FBP) method [5-14]. To remove the noise and eliminate the image blur caused by the data loss during data acquisition, the projections should be first filtered in the frequency domain. The typical filter is the ramp filter, which can effectively eliminate some noise introduced during the imaging process. However, the image detail corresponding to the high frequency is also removed. Therefore, it is necessary to weigh the noise and the image details when choose a filter such as a rectangular window, Hanning window, Hamming window or flat top window. When the FBP algorithm is popularized, many other algorithms for terahertz CT are also proposed. For example, simultaneous algebraic

reconstruction technique (SART), Ordered Subsets Expectation Maximization (OSEM) [25], Modified simultaneous algebraic reconstruction technique (MSART) [26] and Algebraic Reconstruction Technique (ART) [27]. The development of different reconstruction algorithms used in THz CT is presented in the following.

In 2011，B. Recur et al. compared the images reconstructed by FBP, SART and OSEM algorithms from the same projections [25]. The sample is two metallic bars (the diameter D = 12 *mm*) separated by a distance of 50 *mm*. The cross-section of the sample, shown in Fig. 5(a), is simulated according to the real sample. The projections have an angle range of 180° and the projection number is 72. The images reconstructed by FBP, SART and OSEM algorithms are shown from Fig. 5(b) to (d). The results demonstrated that all of reconstructions are blurred compared with the ones in Fig. 5(a). Besides, beam hardening artifacts occur in the images reconstructed by FBP algorithm and SART, which is removed in the image reconstructed by OSEM algorithm.

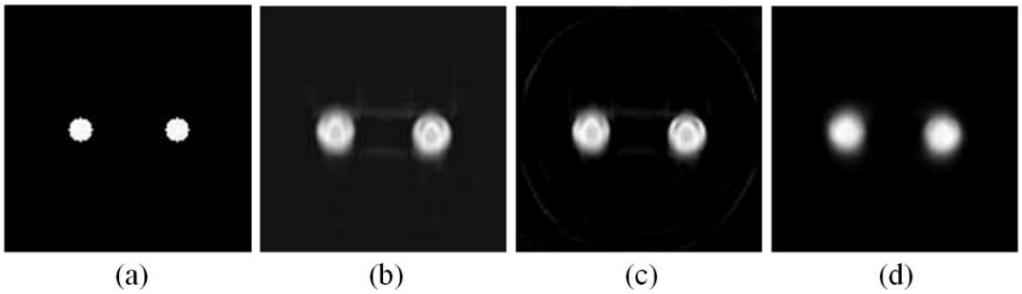

Fig. 5 Cross sections of two metallic bars (12*mm* diameter) separated by 50 *mm*. (a) Ideal cross section simulated according to the sample. (b) FBP reconstruction from detected sinogram. (c) SART reconstruction from detected sinogram. (d) OSEM reconstruction from detected sinogram. (b) to (d): same scale as in (a).

In 2012, Q. Li et al. pointed out that the reconstruction obtained by the SART presents higher quality image than the OSEM algorithm when the projections are insufficient. However, SART algorithm also has many shortcomings, such as the edge effects and high-frequency noise [26]. Therefore, they proposed MSART, which can greatly reduce the edge effect, but high-frequency noise is still existing in the reconstructed image. Therefore, they proposed that applying Gaussian low-pass filtering in the reconstruction process, which can shorten the acquisition time significantly and ensure the image quality.

The beam in X-ray CT system can be considered as a ray for simplifying the reconstruction process. However, the beam in THz CT system is close to Gaussian distribution, which will introduce distortions to the reconstruction if the beam is simplified to ray model. Hence, B. Recur et al. applied Gaussian beam model to the FBP, SART and OSEM algorithms [28]. As shown in Fig. 6(a), the sample composed of four metallic bars (two bars diameter 10*mm* on the top and on the left, one bar diameter 12*mm* on the right and one bar diameter 8mm on the bottom). Three subfigures shown in the first row of Fig. 6(b) are reconstructed from ideal sinograms by the standard FBP, SART and OSEM algorithms. The ones in the second row are reconstructed from

the sinograms obtained simulated on considering the Gaussian beam propagation by the standard FBP, SART and OSEM algorithms. Clearly, the reconstructed bars display elliptical distortion. The images in the end row are reconstructed by three optimized reconstruction methods on considering the Gaussian beam propagation. The reconstructed bars in the last three images are almost identical to the metal bars obtained from the ideal sinogram (first row), which demonstrates that Gaussian beam models can effectively eliminate image distortion introduced by Gaussian beams during imaging.

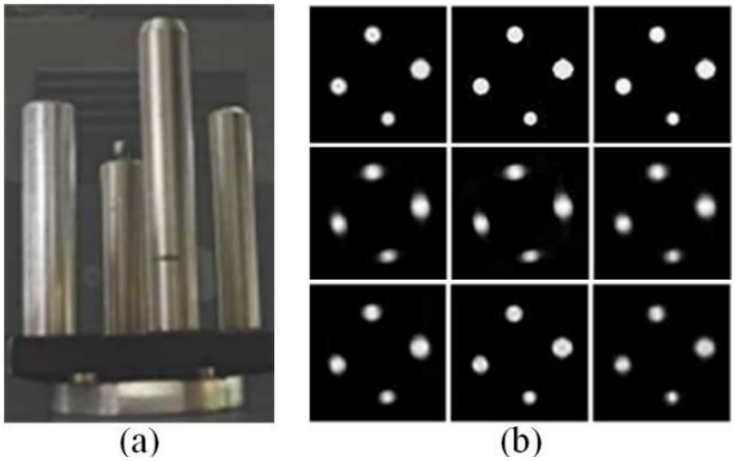

Fig. 6 (a) Object composed of four metallic bars (two bars diameter 10mm on the top and on the left, one bar diameter 12*mm* on the right and one bar diameter 8mm on the bottom), (b) cross-section images: The first row are reconstructed from ideal sinogram, the second row are reconstructed from simulated sinogram on considering Gaussian beam propagation, the end row are reconstructed from detected sinogram.

In 2014, B. Recur optimized the Ordered Subsets Convex (OSC) implementation of the maximum likelihood for transmission tomography (ML-TR) by taking into account Gaussian beam propagation and the intensity distributions of both blank calibration scan and dark-field measured on THz detectors [29]. To conform the quality of images reconstructed by this method, a spray head shown in Fig. 7(a) are detected and the images reconstructed by OSC method are compared with the ones reconstructed by FBP algorithm and SART on considering the beam propagation in Fig. 7(b). A set of 6 cross-sectional images along the y-axis obtained by the standard BFP, SART and the new method combining MLEM and OSC, respectively. Clearly, the cross-section images reconstructed by FBP algorithm are surrounded by many artifacts because the FBP algorithm is particularly sensitive to the noise and it is unable to reconstruct accurately from a few number of projections. Even though the cross-section images reconstructed by SART seem to have better quality, streak artifacts still exist in the fifth subfigure. Moreover, several parts such as the base and outer surface of the object cross section are not reconstructed. The new method proposed in this reference leads to better reconstructions, in which both the inner and outer parts of the object are recovered with high quality.

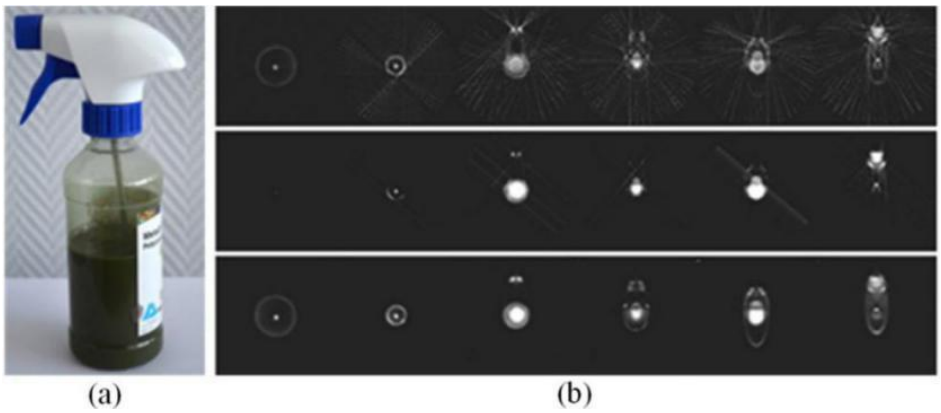

Fig. 7 (a)picture of a spray，(b) Few cross-sections along y-axis of the object obtained respectively by FBP, SART, new method combining MLEM and OSC (from the first to the last line, respectively).

Another method that weakens the influence of beam intensity distribution is replacing the Gaussian beam with a zero-order Bessel beam because zero-order Bessel beam possesses the non-diffraction property over a finite range and is close to the ray model in THz CT reconstruction algorithms [30].

The THz spectral CT can obtain the sample structure and determine the sample material composition. However, most kinds of substances have broad absorption spectra without characteristic peaks and require more elaborate methods [31]. The reference [31] pointed out that continuous wavelet transform (CWT) detection algorithm can provide additional information about the shape of the peaks to improve the substance identification. Hence, the combination of THz spectral CT and CWT will develop the application of THz spectral CT. Subsequently, CWT are applied to Local Reconstruction of THz images by L. Gladden [32].

All of algorithms acquire enough projections and the projection data at all angles evenly spaced over 360, which cannot be satisfied in many applications, so the images reconstructed by these algorithms suffer from a systematic geometric distortion and severe streaking artifacts. More algorithms applied in THz CT should be investigated to remove the aforementioned artifacts and popularize the applications of THz CT.

3. THz time-of-flight imaging

THz time-of-flight (TOF) imaging, one of the earliest THz tomography technology [33], can reconstruct the 3D spatial structure of a sample from the temporal delay of the pulses reflected from the interfaces between.

The principle of TOF imaging is illustrated in Fig. 8. The details of the multilayer structure can be inferred from the pulses partially reflected from each interface because of the discontinuity of the refractive index between two adjacent layers of a multilayered structure.

If the THz pulse is normally incident on the sample, the delay of the reflected pulse $\Delta t = 2n_g d / c$. Here, n_g 、 d and c are the refractive index, the thickness of each layer, and the speed of light, respectively. If the refractive index of the layers is known, d can be determined as follows by measuring the delay time of each pulse, i.e., $d=c\Delta t/2n_g$. This can readily be extended to samples where the THz pulse is incident on the sample at an angle θ, as follows $d=c\Delta t\cos\theta/2n_g$. The resolution depends on the width of the incident THz pulse, and is improved when the pulse is short. When the THz pulse is not ideal (e.g., a top-hat function) and it varies with time in some analogous manner, it would be difficult to distinct the reflected pulse because of the ghost interfaces appearing in the tomographic image. The ghost interfaces could be eliminated by using signal processing, for example by employing deconvolution algorithms [34].

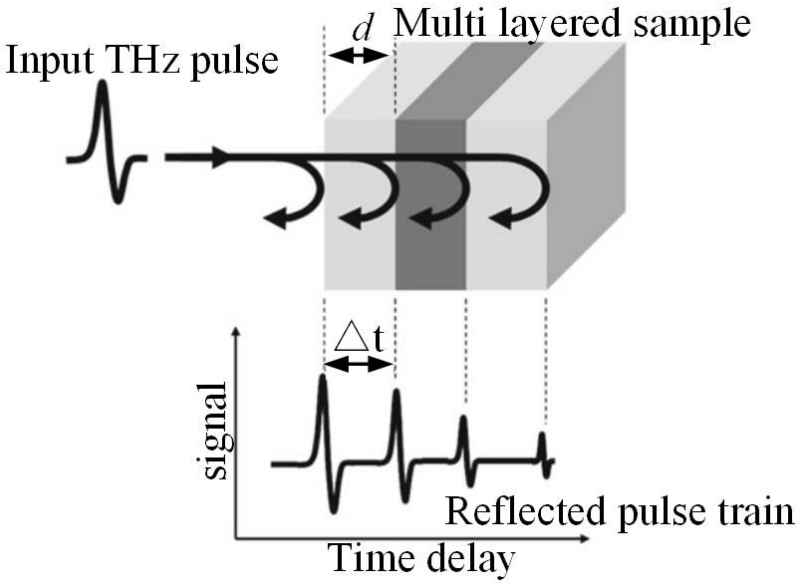

Fig. 8 Principle of TOF-THz tomography

The time-consuming for proceeding two-dimensional (2D) mechanical scanning for the time delay between the THz and the optical probe pulses is significant. One method that reduces data acquisition time is time-to-space conversion by noncollinear two-dimensional free-space electrooptic sampling (2D-FSEOS) [35]., as shown in Fig. 9 [36]. Another method to improve the measurement speed is to choose the faster THz TDS based on asynchronous optical sampling (ASOPS) [5] or electronically controlled optical sampling (ECOPS) [37], which operates without a mechanical delay.

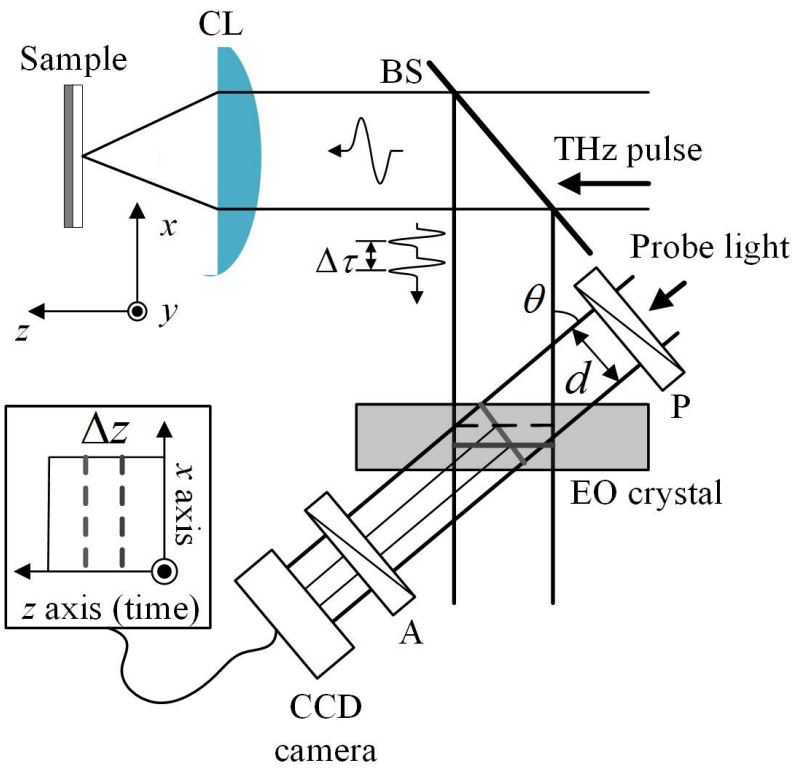

Fig. 9 Principle of real-time THz tomography, CL: cylindrical lens，BS: beam splitter，P: polarizer, A: analyzer, CCD: charge-coupled- device camera.

In 2001, J．L．Johnson introduced Michaelson interferometer to THz TOF imaging. The depth resolution was enhanced to12.5 μm via the Gouy phase shift between the two arms of the interferometer [38]. But the depth resolution should be enhanced for multi-layer structures with a layer thickness of less than 10 μm. In 2008, 4-dimethylamino-N-methyl-4-stilbazolium tosylate (DAST) was pumped by high-peak-power 17-*fs* ultrashort-pulse fiber laser to produce ultra-broad terahertz pulses. By applying these broadband THz pulses to THz TOF imaging, the thickness of 5-μm thin Teflon film was measured correctly [39].

When the gap between layers is small, the signal reflected on the upper layer interferes with that on the lower layer, which degrades the quality of the reconstructed tomographic image in the lower layer. To improve the quality of the lower-layer tomographic image, H. Park et al. proposed a method of interference cancellation between layers to enhance terahertz reflection tomographic imaging performance [40]. In the same year, A. Redo-Sanchez et al. applied the Probabilistic Pulse Extraction (PPEX) algorithm to THz TOF imager and successfully extracted textual content from a packed stack of paper pages without human supervision.

The applications of THz TOF imaging have been further promoted with the enhancing of its depth resolution. For example, THz TOF imaging has been developed to evaluate penetration of cosmetic liquid [41]. As shown in Fig. 10 (a), a silicon on sapphire (SOS) substrate is applied as the sensing plate. The skin sample is put on a “sensing plate” and then cosmetic liquid was

dropped on the surface of the sensing plate. The generated terahertz pulses in the sensing plate are partially radiated into free space directly (The 1st pulse) and the rest of the THz pulses are reflected at the boundary between penetrated and none-penetrated region in the skin (2nd pulse). When the cosmetic liquid is penetrated deeper into the skin sample, the boundary between penetrated and none-penetrated regions is approaching to the sensing plate surface. Thus the penetration depth of the cosmetic liquid can be estimated by measuring the difference in the arrival timing of the first pulse and the second pulse. Fig. 10 (b) shows another similar study, a face mask was set on the sensing plate surface as a reservoir of the cosmetic liquid and the horny layer side of the skin was contacted on the face mask. Thus the penetration depth of the cosmetic liquid is evaluated through the face mask. For this experiment, on the contrary to the previous work, the distance between the surfaces of the sensing plate and the liquid boundary increases by penetration of the cosmetic liquid, thus the time difference of the first and second pulses increases simultaneously. In this investigation, the penetration depth of the cosmetic can be determined according to the time difference between the two pulses, while the penetration speed of the cosmetic can be determined according to the change speed of the time difference. Here, chicken skin is used to simulate human skin, a similar study of pig skin more closer to human skin is underway [41].

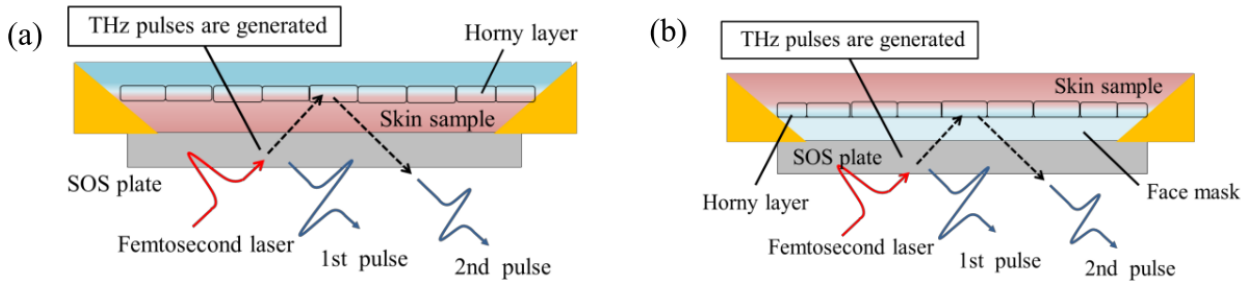

Fig. 10 (a) THz TOF testing the penetration of the cosmetic, (b) THz TOF testing the penetration of the cosmetic when the skin was contacted on the face mask

Earlier this year, K. Rügener et al. proposed that THZ TOF imaging could be used to detect damages on wood caused by insects like the typographer, whose burrows are close to the surface of the wood. This method can assess whether a single tree in the forest is damaged and only the infected trees is removed [42, 43], which can effectively preserve forest plants.

Up to now, the depth resolution of THz TOF imaging technology has achieved micro level [39, 40] and the data acquisition rate is up to KHz [36, 37]. For a region of 100 × 100 × 7.8 mm^3, it takes only 40 seconds to obtain a 3D image of 200 × 200 × 725 voxels [44]. Compared to THz CT, THz time-of-flight imaging does not require the sample rotating, which greatly reduces imaging time and provides high depth resolution. THz TOF can be applied to monitor the oil pollution in water [45], artworks detection [46], defect identification [47], analysis of coating structures and interfaces in solid oral dosage forms [51], quality measurement of automobile paints [52].

4. Conclusions

In conclusion, the development of THz CT and THz TOF imaging is introduced. Since these imaging techniques are proposed, there are two key indicators that are optimized by researchers. One indicator is the data acquisition time, which could be reduced by introducing nonlinear 2D-FSEOS to the imaging system or choosing the faster THz TDS based on ASOPS /ECOPS. The other indicator is the imaging resolution, which could be enhanced by choosing high-frequency THz wave or the optimized reconstruction methods. Besides, the beam model on considering Gaussian beam propagation or replace the Gaussian beam by a zero-order Bessel beam can improve the images' quality. The applications of THz CT and THz TOF imaging in artworks detection, defect identification and industrial inspection are gradually popularizing in practice.

References

[1] X. Zheng, C. Liu. "Recent development of THz technology and its application in radar and communication system". *Journal of Microwaves*, 27(1):1-5 (2011)

[2] S. Hunsche, M. Koch, I. Brener, et al. "THz near-field imaging". *Optics Communications*, 150(1–6): 22-26 (1998)

[3] B. Ferguson, S. Wang, D. Gray, et al. "T-ray computed tomography". *Optics Letters*, 27(15):1312-1314 (2002)

[4] H. Guerboukha, K. Nallappan, and M. Skorobogatiy. "Toward real-time terahertz imaging". *Adv. Opt. Photon.*, 10: 843-938 (2018)

[5] M. Bessou, B. Chassagne, J. P. Caumes, P. Christophe, et al. "Three-dimensional terahertz computed tomography of human bones". *Applied Optics*, 51(28), 6738-6744 (2012)

[6] J. Mukesh, A. Emmanuel, K. Takayuki, et al. "Fast three-dimensional terahertz computed tomography using real-time line projection of intense terahertz pulse". *Opt. Express*, 21, 2423-2433 (2013)

[7] A. Younus, J. P. Caumes, S. Salort, et al. "A continuous millimeter-wave imaging scanner for art conservation science". *Advances in Optical Technologies*, 2011, 1-9 (2011)

[8] D. J. Roth, S. Reyesrodriguez, D. A. Zimdars, et al. "Terahertz computed tomography of NASA thermal protection system materials". AIP Conference. American Institute of Physics, 2012.

[9] S. R. Tripathi, Y. Sugiyama, K. Murate, et al. "Terahertz wave three-dimensional computed tomography based on injection-seeded terahertz wave parametric emitter and detector". *Optics Express*, 24(6), 6433 (2016)

[10] B. Li, D. Wang, X. Zhou, et al. "Terahertz computed tomography in three-dimensional using a pyroelectric array detector". Holography: Advances and Modern Trends V. International Society for Optics and Photonics, 2017.

[11] Y. W. Kim, N. Kim, J. M. Hwang, et al. "Computed tomography image using sub-terahertz waves generated from a high-Tc superconducting intrinsic josephson junction oscillator". *Applied Physics Letters*, 104(8), 26 (2014)

[12] K. Lien Nguyen, L. Johns Michael, F. Gladden Lynn, et al. "Three-dimensional imaging with a terahertz quantum cascade laser". *Opt. Express*, 14, 2123-2129 (2006)

[13] A. Brahm, M. Kunz, S. Riehemann, et al. "Volumetric spectral analysis of materials using terahertz-tomography techniques". *Applied Physics B: Lasers and Optics*, 100(1), 151-158 (2010)

[14] M. Imamura, S. Nishina, A. Irisawa, et al. "3D Imaging and analysis system using terahertz waves". Infrared Millimeter and Terahertz Waves (IRMMW-THz), 2010.

[15] E. Abraham, Y. Ohgi, M. Minami, et al. "Real-time line projection for fast terahertz spectral computed tomography". *Optics letters*, 36(11): 2119-2121 (2011)

[16] T. Yasui, E. Saneyoshi and T. Araki. "Asynchronous optical sampling terahertz time-domain spectroscopy for ultrahigh spectral resolution and rapid data acquisition". *Applied Physics Letters*, 87(6): 061101 (2005)

[17] N. Rothbart, H. Richter, M. Wienold, et al. "Fast 2-D and 3-D terahertz imaging with a quantum-cascade laser and a scanning mirror". *IEEE Transactions on Terahertz Science and Technology*, 3(5):617-624 (2013)

[18] D. Shimao, S. Ichihara, H. Sugiyama, et al. "Radial Digital Breast Tomosynthesis Using a Shift-and-Add Algorithm". *World Congress on Medical Physics and Biomedical Engineering*, 862-865 (2009)

[19] T. Mohr, A. Herdt, and W. Elsässer. "2D tomographic terahertz imaging using a single pixel detector". *Optics express*, 26(3): 3353-3367 (2018)

[20] E. Abraham, A.Younus, C. Aguerre, et al. "Refraction losses in terahertz computed tomography". *Optics Communications*283(10): 2050-2055 (2010)

[21] A. Brahm, A. Wilms, M. Tymoshchuk, et al. "Optical Effects at projection measurements for Terahertz tomography". *Optics & Laser Technology*, 62: 49-57 (2014)

[22] S. Mukherjee, J. Federici, P. Lopes, et al. "Elimination of Fresnel reflection boundary effects and beam steering in pulsed terahertz computed tomography". *Journal of Infrared, Millimeter, and Terahertz Waves*, 34(9), 539-555 (2013)

[23] A. Duhant, M. Triki and O. Strauss. "Terahertz Differential Computed Tomography: a Relevant Nondestructive Inspection Application". *Journal of Infrared, Millimeter, and Terahertz Waves*, 40(2), 178-199 (2019)

[24] J. Pearce, H. Choi, D. Mittleman, et al. "Terahertz wide aperture reflection tomography". *Optics Letters*, 30(13):1653-1655 (2005)

[25] B. Recur, A. Younus, S. Salort, et al. "Investigation on reconstruction methods applied to 3D terahertz computed tomography". *Optics Express*, 19(6):5105-5117 (2011)

[26] Q. Li, Y. D. Li, S. H. Ding et al. "Terahertz computed tomography using a continuous-wave gas laser". *Journal of Infrared, Millimeter and Terahertz Wave*s, 33(5), 548-558 (2012)

[27] Z. Tan, T. Zhou, J. Cao, et al. "Three-dimensional imaging with terahertz quantum cascade laser and quantum well photodetector". *Electronics Letters*, 51(1):85-86 (2015)

[28] B. Recur, J. Guillet, I. Manek-Hönninger, et al. "Propagation beam consideration for 3D THz computed tomography". *Optics Express*, 20(6):5817 (2012)

[29] B. Recur, H. Balacey, S. Bou, et al. "Ordered subsets convex algorithm for 3D terahertz transmission

tomography". *Optics Express*, 22(19):23299 (2014)

[30] A. Bitman, S. Goldring, I. Moshe, et al. "Computed tomography using broadband Bessel THz beams and phase contrast". *Optics Letters*, 39(7):1925 (2014)

[31] A. Brahm, M. Tymoshchuk, F. Wichmann, et al. "Wavelet based identification of substances in terahertz tomography measurements". *Journal of Infrared, Millimeter, and Terahertz Waves*, 35(11), 974-986 (2014)

[32] X. X. Yin, B. W. H. Ng, D. Abbott, et al. "Local Reconstruction for Three Dimensional Terahertz Imaging Using a CW Quantum Cascade Laser". In IPCV, 252-258 (2008)

[33] D. Mittleman, S. Hunsche, L. Boivin, et al. "T-ray tomography". *Optics Letters*, 22(12): 904 (1997)

[34] T. Shibuya, K. Kawase. "Terahertz spectroscopy and imaging". *Infrared & Laser Engineering*, 171(2): 433-449 (2013)

[35] Q. Wu, T. Hewitt, X. Zhang. "Two-dimensional electro-optic imaging of THz beams". *Applied Physics Letters*, 1996, 69(8): 1026-1028

[36] T. Yasuda, T. Yasui, T. Araki. "Real-time two-dimensional spatiotemporal imaging for THz tomography of a moving object". *Optical Terahertz Science and Technology*, TuC6 (2005)

[37] M. Yahyapour, A. Jahn, K. Dutzi, et al. "Fastest thickness measurements with a terahertz time-domain system based on electronically controlled optical sampling". *Applied Sciences*, 9(1283):1-11 (2019)

[38] J. Johnson, T. Dorney, D. Mittleman. "Enhanced depth resolution in terahertz imaging using phase-shift interferometry". *Applied Physics Letters*, 78(6): 835-837 (2001)

[39] J. Takayanagi, S. Kanamori, K. Suizu, et al. "High-resolution terahertz tomography using 17-fs ultrashort-pulse fiber laser". 33rd International Conference on Infrared, Millimeter and Terahertz Waves, 1-2, 2008.

[40] H. Park, J. Son, C. Ahn. "Enhancement of terahertz reflection tomographic imaging by interference cancellation between layers". *Optics Express*, 24(7): 7028-7036 (2016)

[41] T. Morimoto, T. Kuroda, K. Sakai, et al. "Evaluation of Penetration of Cosmetic Liquid with Terahertz Time-Of-Flight Method". 2018 Conference on Lasers and Electro-Optics Pacific Rim (CLEO-PR)

[42] K. Krügener, E.-M. Stübling, R. Jachim, et al. "THz tomography for detecting damages on wood caused by insects". *Applied Optics*, 58(22): 6063-6066 (2019)

[43]https://www.osa.org/enus/about_osa/newsroom/news_releases/2019/terahertz_imaging_technique_reveals_subsurface_ins/

[44] D. S. Yee, K. H. Jin, J. S. Yahng, et al. "High-speed terahertz reflection three-dimensional imaging using beam steering". *Optics Express*, 23(4), 5027-5034 (2015)

[45] W. Sun, X. Wang, Y. Zhang. "A method to monitor the oil pollution in water with reflective pulsed terahertz tomography". *Optik - International Journal for Light and Electron Optics*, 123(21): 1980-1984 (2012)

[46] A. Skryl, J. Jackson, M. Bakunov, et al. "Terahertz time-domain imaging of hidden defects in wooden artworks: application to a Russian icon painting". *Applied Optics*, 53(6): 1033 (2014)

[47] Z. Hua, J. Xu, X. Xu, et al. "Nondestructive defect identification with terahertz time-of-flight tomography".

IEEE Sensors Journal, 5(2): 203-208 (2005)

[48] J. Zeitler, Y. Shen, C. Baker, et al. "Analysis of coating structures and interfaces in solid oral dosage forms by three dimensional terahertz pulsed imaging". *Journal of Pharmaceutical Sciences*, 96(2): 330-340 (2007)

[49] Y. Shen. "Terahertz pulsed spectroscopy and imaging for pharmaceutical applications: A review". *International Journal of Pharmaceutics*, 417(1-2): 48-60 (2011)

[50] J. Zeitler, P. Taday, D. Newnham, et al. "Terahertz pulsed spectroscopy and imaging in the pharmaceutical setting--a review". *Journal of Pharmacy & Pharmacology*, 59(2): 209-223 (2010)

[51] M. Haaser, K. Gordon, C. Strachan, et al. "Terahertz pulsed imaging as an advanced characterisation tool for Analysis of coating structures and interfaces in solid oral dosage forms—A review". *International Journal of Pharmaceutics*, 457(2): 510-520 (2013)

[52] K. Su, Y. Shen, J. Zeitler. "Terahertz sensor for non-contact thickness and quality measurement of automobile paints of varying complexity". *IEEE Transactions on Terahertz Science and Technology*, 4(4): 432-443 (2014)